A Fuel Optimal and Reduced Controller Workload Optimization Model for Conflict Resolution

Adan E. Vela, Senay Solak[†], Eric Feron, Karen Feigh, William Singhose, John-Paul Clarke
Georgia Institute of Technology, Atlanta GA
[†]University of Massachusetts, Amherst MA

Abstract

Despite the existence of several automated air traffic conflict resolution algorithms, there is a need for formulations that account for air traffic controller workload. This paper presents such an algorithm with controller workload constraints modeled parametrically. To this end, we first develop an integer programming model for general conflict resolution, which emphasizes the minimization of fuel costs, and runs in near real-time. A parametric procedure based on this model is then developed to consider controller workload limitations. Two versions of the parametric approach are described, along with computational results. It is demonstrated that both formulations can be used to capture a broad range of possible controller actions.

Introduction

The projected growth in air transportation demand over the next twenty years is likely to exceed the capacity of the unaided air traffic controller. Consenquently the past two decades have seen significant investment in the development of advanced air traffic conflict detection and resolution algorithms. The aim of these algorithms is twofold: to increase capacity and to improve safety. Both the United States Federal Aviation Administration (FAA), and EUROCONTROL, recognize the need to develop support systems for both the tactical (radar controller) and strategic (traffic flow management) controller positions. At the tactical level these systems are particularly important for deconflicting air traffic [1, 2].

The approach presented here seeks to explicitly account for limitations inherent in controller workload, and to devise solutions which are both optimal and which are compatible with controller work practice. Given the difficulty of modeling the aspects of the airspace which contribute to controller workload [3], this is not a trivial task. Hence, conflict resolution models that consider workload issues are rare in the literature despite the existence of several general conflict resolution algorithms. In this study, we develop and utilize a parametric conflict resolution algorithm to account for controller workload issues as accurately as possible. In addition, the algorithm emphasizes the minimization of fuel costs in the resolution of conflicts, and runs in near real-time, making it possible to be implemented as a practical decision aid for air traffic flow management.

The development of our proposed conflict resolution algorithm with an integrated model to account for controller workload involves two phases. In the first phase, we devise a general conflict resolution algorithm, which we refer as *CRP*. This algorithm contains significant improvements over previous integer programming models. Then in the second phase, we develop a parametric procedure to account for controller workload using our conflict resolution model. We define two parameters β and λ, and present two versions of the workload model based on these parameters. By properly setting the values of β and λ, it is possible to drive optimization solutions towards the desired number of conflict resolution commands issued. The two parametric models are referred as $CRP-\beta$ and $CRP-\lambda$.

The conflict resolution algorithm developed in the first phase has several significant contributions, one of which is the modeling of simultaneous speed and heading changes in conflict resolution decisions. Although an algorithm that independently controls either speed or heading changes can be developed through a linear model, consideration of the two types of maneuvers simultaneously results in a highly nonlinear and nonconvex problem. This is mainly due the cost function, which involves fuel burn costs as a function of the airspeed. These relations cannot be represented linearly through the decomposition of the airspeed vector. To overcome the nonlinearity and nonconvexity, we present a model

that makes use of special ordered sets of type two (SOS2). The solution space is segmented into multiple regions, and by using SOS2 variables, a tight convex linear approximation of airspeed can be calculated. The problem can then be cast as a mixed integer linear program, which can be solved in near real-time even for conflicts involving a large number of aircraft. Particular focus has been placed on reducing fuel costs involved in conflict resolution. This was deemed to be important given the significant role that fuel plays in the operating cost of aircraft and the growing concern regarding the impact of gaseous emissions on the environment. Another significant aspect of the proposed approach is the ability to solve a complex problem in near real-time for conflicts involving a large number of aircraft.

A model to account for controller workload is developed in the second phase using a parametric analysis procedure. While the relationship between the layout of the airspace and the traffic density and controller workload are complex and difficult to quantify, there is no doubt that the number of aircraft the controller must monitor and continuously deconflict is a significant driver of controller workload [4, 5]. To this end, we first reformulate *CRP* to include an additional constraint to limit the number of control maneuvers required to resolve a set of conflicts. The bound β on the number of control maneuvers is parameterized, and the problem $CRP-\beta$ is solved for all values of $\beta = 1,\ldots,N$. For the second parametric workload model, $CRP-\lambda$, we introduce an additional cost term in the objective function of *CRP*, namely the L-1 norm of the vector of aircraft maneuvers, weighted by a parameter λ. Ultimately, the two optimization models present formulations that consider the workload costs of resolving traffic. Further, through a comparison of the results over the values of β and λ with observed number of control maneuvers performed by controllers, the parameter values that best reflect the observed conflict resolution procedures can be determined. This would enable the direct use of the developed conflict resolution procedures in any ATM simulation.

In the next section, a brief review of previous conflict resolution algorithms is presented. Then, we describe our conflict resolution algorithm, including the modeling of separation requirements and the linear approximations of the complex fuel cost structures. Afterwards, we discuss the modified versions of the algorithm which are used for considering controller workload limitations, along with the parametric procedure utilized. We then present a simulation methodology for computational tests and the results of these simulations. Finally, our conclusions are discussed.

Background

Conflict detection is the identification of potential conflicts through prediction of future aircraft trajectories based on their current positions, headings, and flight plans. A conflict in air traffic occurs when two or more aircraft encroach the minimum required separation, as defined by some regulatory agency. In most U.S. controlled en route airspace the minimum separation criteria are 5NM. lateral separation and 1,000ft. vertical separation. Presently, once a conflict is detected, it is resolved by a tactical air traffic controller by issuing a clearance to the pilot to change the trajectory, speed or altitude of one or more aircraft so that the minimum separation requirements are satisfied.

Aircraft conflict detection and resolution have been studied extensively. A comprehensive survey of the proposed models is presented in [6]. Since the publication of that survey, several other methods have also been introduced. Among the methods proposed, three of them are directly related to the approach described in this study. These methods contain integer programming models, which enable relatively fast calculations of an optimal conflict resolution procedure. In the first study [7], two integer programming models are developed by allowing all aircraft to perform either speed changes or heading changes, but not both. The objective of the conflict resolution algorithm is defined as the minimization of the maximum deviation of the changes made. The second study [8], a similar integer programming model is discussed. However, the model assumes that only heading changes are allowed to resolve conflict. A third approach [9], considers the problem in three dimensions, and solves for a resolution with only velocity changes using a nonlinear integer programming model, which requires a high level of computational effort.

Conflict resolution algorithms that try to model controller workload issues are few. The authors of [8] utilize an integer programming model to route air-

craft, minimizing the number of conflicts, and thus the workload of the controller. The model is implemented as a conflict detection and resolution procedure. The controller workload is modeled through a knowledge-based approach in [10], where a decision tree structure represents conflict resolution procedures. Although not a direct conflict resolution procedure, a traffic control algorithm is presented in [11] and the algorithm is used to consider controller workload. A somewhat different study is [12], where the authors study the effect of workload on conflict resolution procedures used by controllers.

A Fuel-Optimal Near Real-Time Conflict Resolution Algorithm

There have been two general approaches in the existing conflict resolution studies: rule-based and optimization-based methods. The biggest advantage of rule-based approaches is that they can be implemented in real-time without significant computational effort. Conversely, full nonlinear formulations have limited the applicability of optimization methods. Our approach remedies that shortcoming by developing a model that can be implemented to resolve conflicts in near real-time. This is accomplished by using an efficient integer programming model, which is described in detail below.

Problem Description

Consider a set of *n* aircraft located in a Euclidean plane. Each aircraft *i* is defined by an initial position $\mathbf{p}_i = (x_i, y_i)$, a velocity vector $\mathbf{v}_i^0 = (v_{i,x}^0, v_{i,y}^0)$ defining speed and heading, and a desired final heading θ_i^d. This initial state assumption is valid for en route travel, as the vast majority of en route travel is dominated by steady-state cruising of aircraft.

Each aircraft in the problem is associated with different model types with corresponding fuel burn characteristics. Sample "fuel burn curves" at 33,000 ft (FL330) for three different types of aircraft are shown in Fig. 1, based on data obtained from [13]. In this plot, fuel costs are scaled such that a value of 1 corresponds to the minimum fuel burn for the given aircraft type and flight level. The primary task is to assign each aircraft a single instantaneous heading and speed change at $t = 0$ that provides conflict-free travel, while minimizing a measure of the fuel burn costs over all the aircraft.

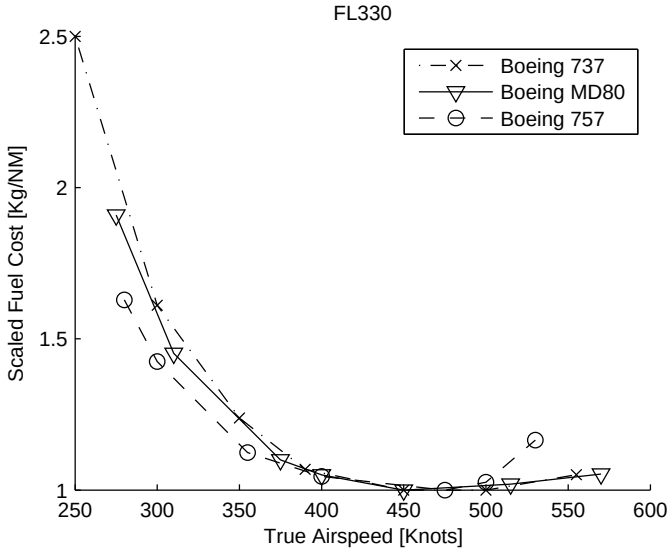

Figure 1: Sample fuel burn curves for three different aircraft models at FL330 [13]

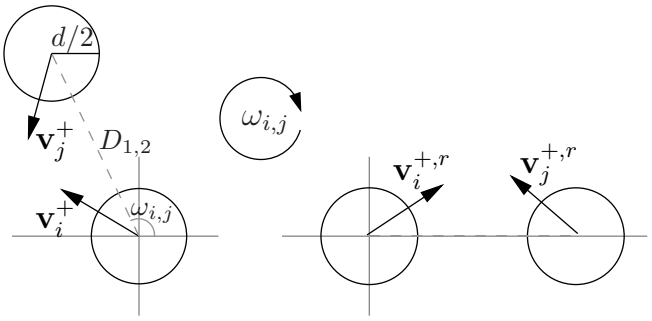

Figure 2: Each aircraft is modeled to have a $d/2$ safety region. To prevent singularities, all pairs of planes are rotated

The trajectory of any aircraft *i* is deemed to be conflict free if the distance between aircraft *i* and any other aircraft *j*, $d_{i,j} = d_{j,i}$, will always be greater than the minimum distance of $d_{i,j}^{min}$. For the purpose of commercial air travel, the nominal minimum separation distance, $d = d_{i,j}^{min}$, between aircraft is 5NM. The minimum separation distance can be visualized by encircling each aircraft with a safety region of radius $d/2$, as shown in Fig. 2. If we assume that trajectories of aircraft are linearly extrapolated in time, then for aircraft *i* and *j* with given trajectories, the necessary minimum separation condition is expressed by the following inequality:

$$\sqrt{x_{dist}^2 + y_{dist}^2} \geq d \quad \forall t \in R^+ \tag{1}$$

where x_{dist} and y_{dist} represent the distance between the two aircraft in the corresponding coordinate axes:

$$\begin{aligned} x_{dist} &= (x_i + v_{i,x}t) - (x_j + v_{j,x}t) \\ y_{dist} &= (y_i + v_{i,y}t) - (y_j + v_{j,y}t) \end{aligned} \tag{2}$$

Over the next few sections, we describe a methodology for formulating a fuel-optimal conflict resolution model that ensures that separation conditions (1) hold for $t \in R^+$. Unlike most models in the literature, the process yields a mixed integer linear programming problem, which is solvable in near real time for dynamic routing decisions.

Before describing the details of the proposed approach, we first list some initialization assumptions. We assume that no aircraft violate the minimum separation conditions (1) at $t = 0$. Also, no initial conditions are such that aircraft are on a collision course that cannot be avoided with control actions over a reasonable time frame.

The model does not take into account the time to execute state changes. It is assumed that the time to complete any maneuver change is small in comparison to the time until conflict. However, the safety region about each aircraft can be expanded to handle uncertainty from resulting maneuver changes, wind variation, or other unmodeled phenomena.

Starting with the initial conditions $\left\{(\mathbf{p}_i, \mathbf{v}_i^0)\right\}$, the solution to the resulting optimization model is the set of new velocity vectors $\left\{\mathbf{v}_i^+\right\}$ for each aircraft. Updated speed and heading commands can then be extracted from $\mathbf{v}_i^+$. The new velocity vector $\mathbf{v}_i^+$ represents the solution for an instantaneous change in the trajectory.

Problem Formulation

For conflict-free trajectories, each pair of aircraft must satisfy separation constraint (1). In this section a basis formulation is presented in which the separation condition is deconstructed into a set of linear constraints that ensure no aircraft encroaches another aircraft's safety region. This approach is similar to the one used in [7] to determine the separation constraints.

Consider a pair of aircraft i and j with initial position and velocity states:

$$\begin{aligned} \mathbf{p}_i = (x_i, y_i), \quad \mathbf{v}_i^0 = \left[v_{i,x}^0, v_{i,y}^0\right]^T \\ \mathbf{p}_j = (x_j, y_j), \quad \mathbf{v}_j^0 = \left[v_{j,x}^0, v_{j,y}^0\right]^T \end{aligned} \tag{3}$$

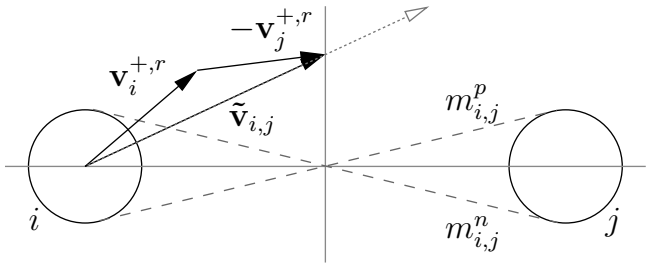

Figure 3: Definition of the safety regions for aircraft

A given aircraft i may alter its trajectory to prevent conflict by changing its velocity vector by $\mathbf{dv}_i = [dv_{i,x}, dv_{i,y}]^T$. Applying $\mathbf{dv}_i$ to each corresponding aircraft defines new trajectories as follows:

$$\mathbf{v}_i^+ = \mathbf{v}_i^0 + \mathbf{dv}_i, \quad \mathbf{v}_j^+ = \mathbf{v}_j^0 + \mathbf{dv}_j \tag{4}$$

To avoid singularities in the problem formulation, the reference frame for the pair of planes is rotated so that the angle $\omega_{i,j} = 0$, where $\omega_{i,j}$ is the angle between the horizon and the connector between the aircraft. This process is demonstrated in Fig. 2. For an initial angle $\omega_{i,j} \in [0, 2\pi)$, rotation is performed by multiplying the initial position and velocity vectors by the rotation matrix $\mathbf{R}(\omega_{i,j})$:

$$\begin{aligned} \mathbf{R}(\omega_{i,j}) &= \begin{bmatrix} cos(\omega_{i,j}) & sin(\omega_{i,j}) \\ -sin(\omega_{i,j}) & cos(\omega_{i,j}) \end{bmatrix} \\ \mathbf{p}_i^r = \mathbf{R}(\omega_{i,j})(x_i, y_i), \quad \mathbf{v}_i^{+,r} &= \mathbf{R}(\omega_{i,j})\mathbf{v}_i^+ \\ \mathbf{p}_j^r = \mathbf{R}(\omega_{i,j})(x_j, y_j), \quad \mathbf{v}_j^{+,r} &= \mathbf{R}(\omega_{i,j})\mathbf{v}_j^+ \end{aligned} \tag{5}$$

Once the rotation is performed, a set of linear constraints to ensure that a pair of aircraft maintain separation is derived from the relative velocity $\tilde{\mathbf{v}}_{i,j}$ and initial position $\tilde{\mathbf{p}}_{i,j}$ of aircraft i and aircraft j, i.e.:

$$\begin{aligned} \tilde{\mathbf{v}}_{i,j} &= \mathbf{v}_i^{+,r} - \mathbf{v}_j^{+,r} \\ \tilde{\mathbf{p}}_{i,j} &= \mathbf{p}_i^{+,r} - \mathbf{p}_j^{+,r} \end{aligned} \tag{6}$$

Conflict between aircraft i and aircraft j occurs when the ray originating from aircraft i extending along $\tilde{\mathbf{v}}_{i,j}$ passes through the safety region around aircraft j. For aircraft with safety regions of radius $d/2$, the projected safety region of aircraft i along $\tilde{\mathbf{v}}_{i,j}$ must remain outside the safety region of aircraft j, as illustrated in Fig. 3.

By understanding the method of ray extension along the relative velocity, the allowable regions for $\tilde{\mathbf{v}}_{i,j}$

can be delineated. Ultimately, the set of lines, $l^p_{i,j}$ and $l^n_{i,j}$, with slopes $m^p_{i,j}$ and $m^n_{i,j}$, tangent to the safety regions of each aircraft is key to defining the linear constraints through the following relation:

$$\begin{aligned} \frac{\tilde{v}_{i,j,y}}{\tilde{v}_{i,j,x}} &\leq m^n_{i,j} \\ \text{or} & \\ \frac{\tilde{v}_{i,j,y}}{\tilde{v}_{i,j,x}} &\geq m^p_{i,j} \end{aligned} \tag{7}$$

For aircraft that are D distance apart, with mandatory separation d, the slopes $m^p_{i,j}$ and $m^n_{i,j}$ are given by:

$$\begin{aligned} m^p_{i,j} &= d/\sqrt{D^2-d^2} \\ m^n_{i,j} &= -d/\sqrt{D^2-d^2} \end{aligned} \tag{8}$$

Constraints (7) can be expressed as linear inequalities by multiplying the right-hand side by the denominator $\tilde{v}_{i,j,x}$, separating the condition $\tilde{v}_{i,j,x} \leq 0$, and removing overlaps in the constraints:

$$\begin{aligned} & \tilde{v}_{i,j,y} \leq \tilde{v}_{i,j,x} m^n_{i,j}, \quad \tilde{v}_{i,j,x} \geq 0 \\ \text{or} & \\ & \tilde{v}_{i,j,y} \geq \tilde{v}_{i,j,x} m^p_{i,j}, \quad \tilde{v}_{i,j,x} \geq 0 \\ \text{or} & \\ & \tilde{v}_{i,j,x} \leq 0 \end{aligned} \tag{9}$$

The separation constraints (9) are expressed as linear inequalities of the decision variables $\tilde{v}_{i,j,x}$ and $\tilde{v}_{i,j,y}$, which are functions of the speed and heading changes, $\mathbf{dv}_i$. Furthermore, the condition $\tilde{v}_{i,j,x} \leq 0$ allows for the case of aircraft trailing one another, i.e. the singularity of $\tilde{v}_{i,j,x} = 0$ in the slope is admissible for this formulation. The constraints (9) are then applied to all pairs of aircraft. As the constraints are reciprocal, only one set of constraints is required for each pair. Because all pairs of aircraft are resolved simultaneously for all future time, there are no secondary conflicts. In line with the primary goal of providing a framework in which fuel costs are considered in conflict resolution and aircraft routing, an appropriate cost function $G_0(\mathbf{s},\theta)$ can be defined as:

$$G_0(\mathbf{s},\theta) = g_s(\mathbf{s}) + g_h(\theta) \tag{10}$$

where g_s and g_h are nonlinear scalar functions of the airspeeds $\mathbf{s}$, and the headings θ of the aircraft. The function g_s measures the fuel burn percentage of an aircraft, while g_h accounts for the scaled increase in distance traveled due to a deviation from the desired route, and the estimated cost to return to the desired path. Considering both parts, G_0 is the fuel consumption percentage with respect to the optimal path at a desired airspeed when there are no obstacles for all aircraft.

The measures $\mathbf{s}$ and θ are nonlinear nonconvex functions of the decision variables $\mathbf{dv}_i$. In the following sections, we develop tight convex linear approximations for the cost functions $g_s(\mathbf{s})$ and $g_h(\theta)$, and show that the underlying optimization problem can be modeled as a linear integer programming problem.

Previous conflict resolution research described in the introduction focused on minimizing the required velocity deviation, $\mathbf{dv}_i$, to ensure separation. Noting that any such deviation incurs costs, a measure of airspeed is required to provide a broader framework to understand and study the fairness and costs associated with aircraft routing. The final airspeed of aircraft i, s^+_i, can be calculated according to a first-order approximation:

$$s^+_i \sim s^0_i + \frac{1}{s^0_i}[v^0_{i,x} v^0_{i,y}]\mathbf{dv}_i = \hat{s}_i \tag{11}$$

While a first-order approximation is satisfactory for $\mathbf{dv}_i$ when $\left\|\mathbf{dv}_i \times \mathbf{v}^0_i\right\| \sim 0$, the approximation degrades as larger heading angle changes are required to avoid conflicts. For heading deviations of 15° and greater, error from a first-order estimate of airspeed diminishes the ability of any formulation to utilize the approximation to effectively solve for fuel-optimal routing.

To overcome the shortcomings of a first-order approximation, constraints making use of Special Ordered Sets of Type 2 (SOS2) can provide a more accurate approximation of airspeed. SOS2 variables are a set of non-negative continuous variables such that, at most, one pair of consecutively indexed variables is nonzero. Hence, if $\lambda_1,\ldots,\lambda_n$ is SOS2, and if $\lambda_i \geq 0$, then either $\lambda_{i-1} \geq 0$ or $\lambda_{i+1} \geq 0$ and all other $\lambda_j = 0$. Although introduction of SOS2 variables into the optimization model adds to the complexity of the formulation, it enables a much better approximation of the airspeed over the feasible region.

Consider an aircraft with some initial heading θ^0, and which can perform heading changes of $\pm d\theta$ to ensure separation. We assume that the range of possible final heading values is broken into m adjacent regions according to the set $\theta = \{d\theta_1 + \theta^0, \ldots, \theta^0, \ldots, d\theta_m + \theta^0\} = \{\theta_1, \ldots, \theta_m\}$. These regions need not be uniform in size. A grid structure over the feasible space is then formed including the origin, and the set $(X_q, Y_q) = \left\{v_i^{max} cos(\theta_q), v_i^{max} sin(\theta_q)\right\}, \quad \forall q \in \{1, 2, \ldots m\}$. The function $Z_q = \left\|\mathbf{v}_q\right\|$ is then evaluated over the grid points. The airspeed estimate, $\hat{s}_i$, is calculated by forming a convex combination of the function values of the grid points associated with the sector encompassing $\mathbf{v}_i^+$. The airspeed is given by the following set of constraints:

$$\begin{aligned} \hat{v}_{i,x}^+ &= \sum_{q=0}^{m} X_q \lambda_q \\ \hat{v}_{i,y}^+ &= \sum_{q=0}^{m} Y_q \lambda_q \\ \hat{s}_i &= \sum_{q=0}^{m} Z_q \lambda_q \\ \\ \sum_{q=0}^{m} \lambda_q &= 1 \\ \lambda_q &\in \text{SOS2} \quad \forall q \end{aligned} \tag{12}$$

The SOS2 approximation yields a much tighter approximation over the domain, as shown in Fig. 4. For the example provided, using only four regions spread over ± 45 degrees around the initial heading, the largest percent error between the approximation and the actual airspeed is only 2%. In comparison, the linear approximation in (11) increases to approximately 30% at 45°.

For cost calculations due to airspeed changes, we assume that the airspeed cost for each aircraft is the percent deviation in fuel burn, per unit distance traveled, when compared to the optimal speed of the aircraft. Given the fuel burn per minute as a function of the true airspeed, this value can be converted to fuel burn per NM traveled by dividing by the ground speed.

Given a set with different aircraft models, it is important to consider the fuel burn equations for each model type. For each aircraft model, we define a set of l linear inequalities defined by slopes $a_{k,i}$ and intercepts

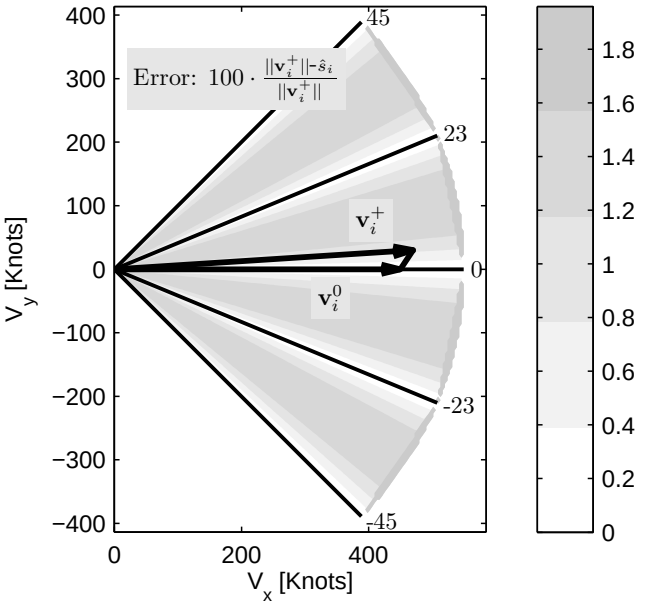

Figure 4: Percent error in the SOS2 approximation of airspeed

$b_{k,i}$ for $k = 1, \ldots, l$, based on fuel curves such as the ones in Fig. 1. These inequalities are then used to formulate the approximate convex fuel cost, t_i, for the i^{th} aircraft:

$$\begin{aligned} a_{1,i}\hat{s}_i + b_{1,i} &\leq t_i \\ a_{2,i}\hat{s}_i + b_{2,i} &\leq t_i \\ &\vdots \\ a_{l,i}\hat{s}_i + b_{l,i} &\leq t_i \end{aligned} \tag{13}$$

The fuel cost associated with a heading angle deviation and a return to the desired flight path is approximated using a two step process that is illustrated in Fig. 5. In the first step, the aircraft makes a heading angle change to resolve conflict. Then in the second stage, the heading is corrected back towards the destination, as soon as the aircraft is clear from the conflict. In conjunction with conflict detection methods, we assume that there exists a complete knowledge of the system. Particularly, we assume that conflict detection methods can predict the largest distance $d_{i,1}$, for a possible conflict between aircraft i with another aircraft assuming no corrective action is taken, where $d_{i,1}$ is illustrated in Fig. 5. Let $D_i = d_{i,1} + d_{i,2}$ designate the straight-line distance between the destination and the current position of the airplane i.

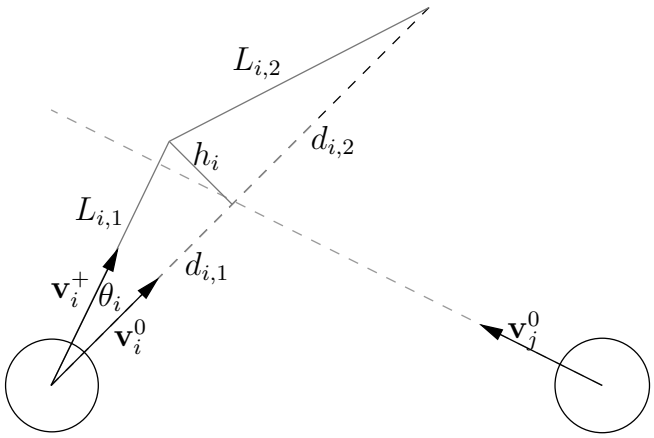

Figure 5: Heading angle deviations increase the resulting distance traveled as calculated by $L_{i,1}+L_{i,2}$

If maintaining separation requires a heading angle change, then the travel distance is $L_{i,1}+L_{i,2}$, and the normalized increase $D_{p,i}$ in the travel distance is:

$$D_{p,i} = (L_{i,1}+L_{i,2})/D_i \tag{14}$$

The next step is to establish a relationship between the change in the heading angle and the resulting increase in fuel cost. Making use of the heading change $d\theta_i$ instead of $L_{i,1}$ in (14) and applying the law of cosines to solve for $L_{i,2}$ over the range $d\theta_i \in (-\pi/2, \pi/2)$, $D_{p,i}$ can be represented as:

$$D_{p,i}(d\theta_i) = \frac{\frac{d_{i,1}}{cos(d\theta_i)} + \sqrt{\left(\frac{d_{i,1}}{cos(d\theta_i)}\right)^2 + D_i^2 - 2d_{i,1}D_i}}{D_i} \tag{15}$$

where the first term in the numerator corresponds to $L_{i,1}$, and the second term corresponds to $L_{i,2}$.

Assuming that any heading angle change allows the aircraft to fly near the optimal fuel burn speed, the additional distance can be used as a fuel consumption measure. To integrate this measure, we develop a tight linear approximation of the relation in (15). Note that (15) is a convex function in the interval $d\theta_i \in (-\pi/4, \pi/4)$, yet nonconvex in the decision variables $\mathbf{dv}_i$. A contour plot of $D_{p,i}$ as a function of the airspeed changes $\mathbf{dv}_i$ is given in Fig. 6. Thus, a linear approximation is possible by fitting a set of $2q$ planes between angles $[\theta_{-q}, \ldots, \theta_0, \ldots, \theta_q]$ to (15). Each plane w, approximating (15) within some interval $[\theta_w, \theta_{w+1}]$, can be

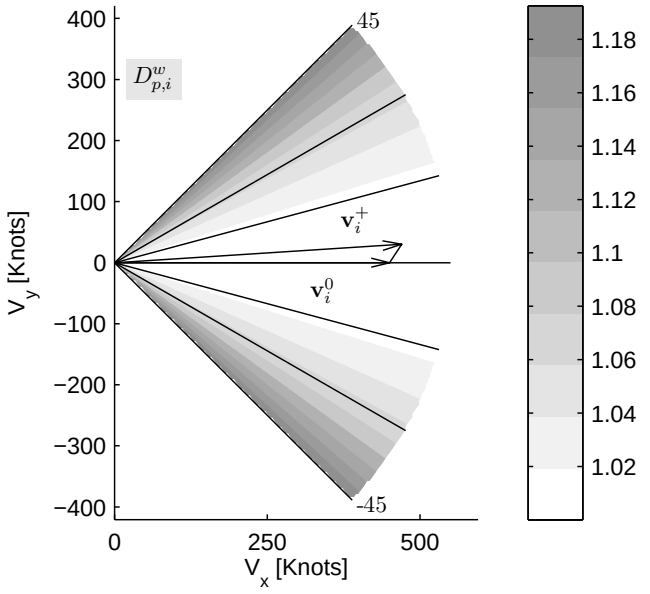

Figure 6: Contour plot of the normalized additional distance traveled for a required heading change

determined by first calculating the points x_w, y_w, z_w and $x_{w+1}, y_{w+1}, z_{w+1}$ as follows:

$$\begin{aligned} x_w &= v_{i,max} cos(\theta_w) \\ y_w &= v_{i,max} sin(\theta_w) \\ z_w &= D_{p,i}(\theta_w) \\ x_{w+1} &= v_{i,max} cos(\theta_{w+1}) \\ y_{w+1} &= v_{i,max} sin(\theta_{w+1}) \\ z_{w+1} &= D_{p,i}(\theta_{w+1}) \end{aligned} \tag{16}$$

Then, a linear function relating the scaled increase in distance traveled due to a heading deviation $d\theta_i$, where $d\theta_i \in [\theta_w, \theta_{w+1}]$ can be obtained from:

$$\det\left(\begin{bmatrix} x & y & \hat{D}^w_{p,i} - 1 \\ x - x_w & y - y_w & \hat{D}^w_{p,i} - z_w \\ x - x_{w+1} & y - y_{w+1} & \hat{D}^w_{p,i} - z_{w+1} \end{bmatrix}\right) = 0 \tag{17}$$

where $\hat{D}^w_{p,i}$ is the approximate percent increase in distance traveled and $x = v^+_{i,x}$ and $y = v^+_{i,y}$. Note that (17) is a direct result of the points $(x_w, y_w, z_w), (x_{w+1}, y_{w+1}, z_{w+1})$ and $(x, y, \hat{D}^w_{p,i})$ being on the same plane. The resulting relation can be included as a constraint in the optimization model as:

$$\hat{D}^w_{p,i} = c_1 x + c_2 y + c_3 \tag{18}$$

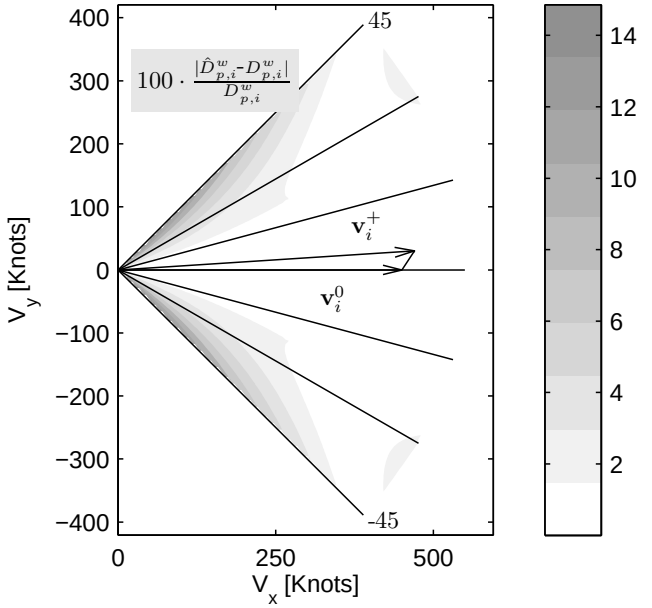

Figure 7: Percent error in the approximation of the scaled additional distance traveled for a required heading change

where c_1, c_2, and c_3 are constants obtained from (17).

As shown in Fig. **??**, the convex planar representation closely approximates $D_{p,i}(d\theta_i)$. The approximation error is less than 1% for most values of the heading angle change within the nominal operating bounds.

Assuming that the aircraft operates at the optimal fuel burn rate when applying a heading change, the additional percentage fuel cost, u_i, due to the heading angle change for the i^{th} aircraft, over the optimal fuel burn rate is equal to the additional percent distance traveled, i.e. $D_{p,i}$.

To implement the planar approximation in the optimization model, the following constraints to define the heading change costs, u_i, for each aircraft is included in the formulation:

$$\hat{D}^w_{p,i} \leq u_i \quad \forall w \tag{19}$$

We assume that the overall objective is a mixture of the minimization of the sum of individual fuel costs, i.e. t_{sum}, and minimization of the maximum fuel burn over all the aircraft, i.e. t_{max} (to ensure that no single aircraft is excessively penalized). Note that the individual fuel costs are equal to the sum of the costs incurred due to the change in airspeed t_i and the costs due to the change in heading angle u_i. Thus, the overall objective function for the problem can be expressed as:

$$f_{fuel} = J_m t_{max} + J_s t_{sum} \tag{20}$$

where J_m and J_s are constants that form a ratio for valuing the minmax or cumulative sum approaches, and can be determined based on the policy that the decision maker wants to implement. The variables t_{sum} and t_{max} are defined in the formulation through the following sets of constraints:

$$\begin{aligned} t_i + u_i &\leq t_{max} \quad \forall i \\ t_{sum} &= \sum_{i=1}^{n} (t_i + u_i) \end{aligned} \tag{21}$$

Hence, the overall formulation for the conflict resolution problem can be summarized as follows:

$$\begin{aligned}
CRP\text{: min} \quad & J_m t_{max} + J_s t_{sum} \\
\text{s.t.} \quad & \\
\tilde{v}_{i,j,y} - \tilde{v}_{i,j,x} m^n_{i,j} &\leq (1 - r^{ij}_1) M^{ij}_1 \quad \forall i < j \\
-\tilde{v}_{i,j,x} &\leq (1 - r^{ij}_1) M^{ij}_1 \quad \forall i < j \\
-\tilde{v}_{i,j,y} + \tilde{v}_{i,j,x} m^p_{i,j} &\leq (1 - r^{ij}_2) M^{ij}_2 \quad \forall i < j \\
-\tilde{v}_{i,j,x} &\leq (1 - r^{ij}_2) M^{ij}_2 \quad \forall i < j \\
\tilde{v}_{i,j,x} &\leq (1 - r^{ij}_3) M^{ij}_3 \quad \forall i < j \\
\hat{D}^w_{p,i} = c^i_1 v^+_{i,x} + c^i_2 v^+_{i,y} + c^i_3 &\quad \forall i \\
\tilde{v}_{i,j,x} = v^{+,r}_{i,x} - v^{+,r}_{j,x} &\quad \forall i < j \\
\tilde{v}_{i,j,y} = v^{+,r}_{i,y} - v^{+,r}_{j,y} &\quad \forall i < j \\
\mathbf{R}(\omega_{i,j}) = \begin{bmatrix} cos(\omega_{i,j}) & sin(\omega_{i,j}) \\ -sin(\omega_{i,j}) & cos(\omega_{i,j}) \end{bmatrix} &\quad \forall i < j \\
\mathbf{v}^{+,r}_i = \mathbf{R}(\omega_{i,j}) \mathbf{v}^+_i &\quad \forall i < j \\
\mathbf{v}^{+,r}_j = \mathbf{R}(\omega_{i,j}) \mathbf{v}^+_j &\quad \forall i < j \\
a_{l,i} s_i + b_{l,i} \leq t_i &\quad \forall l, i \\
t_i + u_i \leq t_{max} &\quad \forall i \\
t_{sum} = \textstyle\sum_{i=1}^{n} (t_i + u_i) &
\end{aligned}$$

$$\begin{aligned}
\textstyle\sum_{k=1}^{3} r^{ij}_k = 1 &\quad \forall i < j \\
v^+_{i,x} = \textstyle\sum_{q=0}^{m} X_q \lambda_q &\quad \forall i \\
v^+_{i,y} = \textstyle\sum_{q=0}^{m} Y_q \lambda_q &\quad \forall i \\
s_i = \textstyle\sum_{q=0}^{m} Z_q \lambda_q &\quad \forall i \\
\hat{D}^w_{p,i} \leq u_i &\quad \forall w, i \\
\textstyle\sum_{q=0}^{m} \lambda_q = 1 & \\
r^{ij}_k \in \{0,1\} &\quad \forall k, i < j \\
s_i, t_i, u_i, t_{max}, t_{sum}, \hat{D}^w_{p,i} \geq 0 & \\
\lambda_q \in \text{SOS2} &\quad \forall q
\end{aligned} \tag{22}$$

For brevity, the above formulation is written as:

$$\begin{array}{ll} \min & G_{base}(\mathbf{v}) \\ \text{s.t.} & \mathbf{v} \in \mathscr{V} \end{array} \tag{23}$$

where $\mathscr{V}$ is the set of feasible maneuvers.

Consideration of Controller Workload

Using *CRP* as the basic problem structure, we define two additional formulations that consider controller workload limitations. The first formulation, $CRP-\beta$, uses some additional binary variables and a parametric bound β to limit the maximum number of deviations allowed for conflict resolution. The second formulation, $CRP-\lambda$, is based on the L_1 norm of the vector of aircraft maneuvers and attempts to approximate the maneuver limitations by adding a penalty function to the cost.

$CRP-\beta$ *Formulation*

In the first workload formulation, we include an additional term to the cost function of *CRP*, as well as some supplementary constraints. These modifications are used to restrict the number of resolution commands that can be used to resolve conflicts.

If β is the maximum number of resolution commands allowed, and κ_i is an additional binary variable to indicate if aircraft i is not being issued a conflict resolution command, then the problem becomes:

$$\begin{array}{lll} CRP-\beta: & \min & G_{base}(\mathbf{v}) + K \cdot R_{total} \\ & \text{s.t.} & \kappa_i \Rightarrow \mathbf{v}_i = 0 \\ & & R_{total} = N - \sum_{i=1}^{N} \kappa_i \\ & & R_{total} \leq \beta \\ & & \mathbf{v} \in \mathscr{V} \end{array} \tag{24}$$

where N is the number of aircraft and K is some non-negative cost coefficient, allowing the inclusion of a penalty function based on the total number of resolution commands.

Inclusion of the binary variables κ_i, and the corresponding constraints increases the computational difficulty of the problem. However, it allows specification of the maximum number of resolution commands. Such a a limitation is a valid approximation for considering limits of controller workload since there is a practical limit to the number of resolution commands a human air traffic controller can issue in a given time frame.

Using $CRP-\beta$ it is also possible to fix the number of aircraft resolutions to a specific value. Furthermore, if the optimization is run in a receding horizon format, such that it is solved at regular time intervals, it can be linked to controller constraints. For example, if a controller is limited to $\bar{L}$ communications every δT minutes, then $\beta = \bar{L}/\delta T$.

$CRP-\lambda$ *Formulation*

Similar to $CRP-\beta$, $CRP-\lambda$ is based on the original formulation with slight modifications to the cost function. We first introduce the variable Γ_i to represent the absolute measure of deviations for each aircraft i. The L_1 norm of the vector Γ, multiplied by the parameter λ is then used to implement a penalty cost for the deviations. As the multiplier λ is increased, the optimization solution will reduce the number of deviations. And at $\lambda \to \infty$, the solution will locally converge to include the minimum possible number of deviations. This formulation can be expressed as:

$$\begin{array}{lll} CRP-\lambda: & min & G_{base}(\mathbf{v}) + \lambda ||\Gamma||_1 \\ & \text{s.t.} & \Gamma_i = ||\mathbf{dv}_i||_1 \\ & & \mathbf{v} \in \mathscr{V} \end{array} \tag{25}$$

The formulation above is a relaxation of the $CRP-\beta$, as the number of allowable maneuvers is not bounded. It has some key benefits, as it balances fuel cost savings to the number of resolution commands that can be issued at any time. Because it does not fix the number of resolutions, it is always guaranteed to be feasible, assuming the *CRP* is feasible. Furthermore, note that the formulation does not require the addition of new binary variables or complicating constraints. As a result, $CRP-\lambda$ can be solved in the same time magnitude as the base CRP formulation.

Simulation and Results

In this section, we describe the methodology used in computational testing of the two workload formulations, and present a comparison of the two algorithms. The objective of the computational tests is to analyze the effects of the parameter β and λ on the conflict resolution procedure, and assess the ability of the formulations to provde results consistent with expected controller decisions. To this end, we study the performance

of the two workload formulations through a series of randomly generated scenarios based on current air traffic conditions, with varying levels of traffic volumes.

Simulation Methodology

The computational tests implements the formulations in a realistic setting based on air traffic patterns in sector ZME19 within the Memphis Air Route Traffic Control Center. Single flight-level traffic loads up to 13 aircraft at the median peak levels were used to demonstrate that the proposed algorithm can be implemented in real operational situations. These realistic tests were conducted dynamically in a receding horizon format to simulate directing traffic through the sector. The conflict resolution problem was solved in 30 second intervals if a new aircraft arrived during the time period. Otherwise, the resolution problem was solved nominally every 5 minutes. The simulations were stopped when all generated arrivals cleared the sector.

To approximate traffic through the sector, a statistical distribution of entry-exit pairs was generated using historical data of aircraft traveling through the center at and above FL300 during the 24 hour period of September 1, 2005. The sector boundary was broken up into 10NM segments, which were numerically identified as entrances and exits. For the distribution, each aircraft was designated to enter and exit through a particular boundary segment. Aircraft interarrival times into the sector were assumed to follow an exponential distribution with a slight modification such that aircraft entering at the same entrance had a minimum time separation of 2 minutes.

To increase traffic loads, the average interarrival time between aircraft was decreased. For simulations, the average interarrival time between aircraft was taken at $[2,3,4,\ldots,10]$ minutes between aircraft. For each arrival-rate, 10 samples were taken with 200 aircraft each. The median peak number of aircraft in the sector for each arrival rate is shown in Fig. 8. Aircraft models were also assigned according to a sampled distribution taken from the historical data. The aircraft span a broad range, including regional, narrow body, wide body, and business class jets. All sampled aircraft trajectories provided to the simulation were assumed to be flying east to west at FL360, consistent with the current traffic pattern in the sector. An example of the sampled traffic

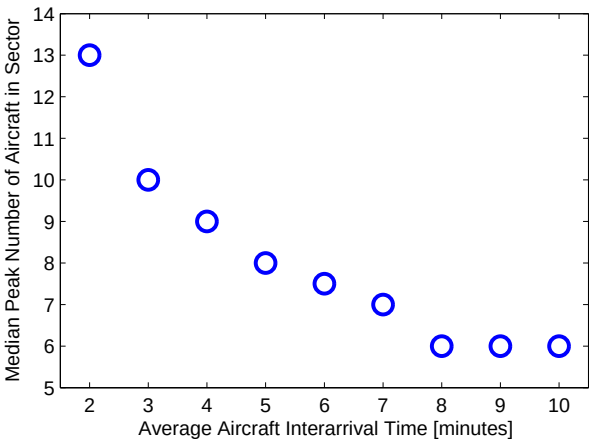

Figure 8: Median peak number of aircraft in the sector for each arrival rate

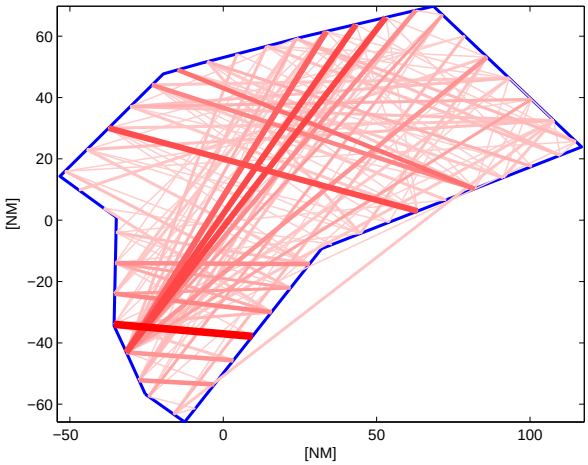

Figure 9: Distribution of en route flights in ZME19

pattern through the sector is displayed in Fig. 9. The darker and thicker lines in the figure correspond to entry-exit pairs that are used more frequently.

The simulations were performed similar to a near-real time implementation, where the problem was solved multiple times for a stream of 200 aircraft entering the sector. While $CRP-\lambda$ is implemented as presented in its formulation, a more complex procedure is used for $CRP-\beta$ to ensure feasibility. In the simulation runs, the parameter β was defined as the upper bound on the number of resolutions commands issued in a 5 minute interval. Initially, as new aircraft enter the sector, the minimum number of aircraft are issued commands to resolve any conflicts by assigning a large value to weight

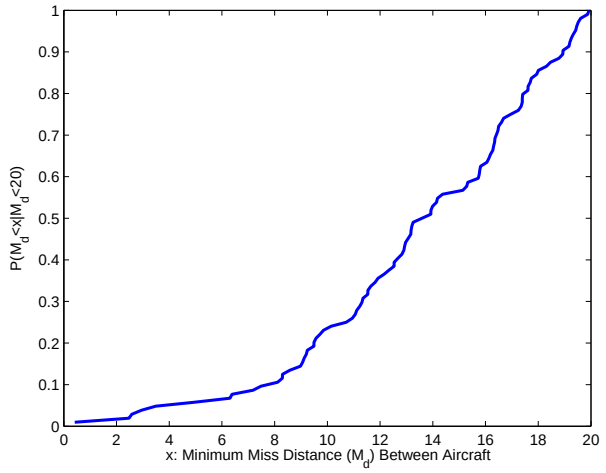

Figure 10: Distribution of minimum aircraft miss distances from historical data

K in the model. Then, the number of issued resolutions during the 30 second interval is subtracted from β. If the number of remaining maneuvers is insufficient to solve the resolution problem at each 5 minute update, then the minimum resolution solution with a large value of K is applied once again to resolve conflicts.

While the nominally required separation between aircraft is 5NM, the simulations were performed with a spacing requirement of 8NM to better replicate en route conditions and controller actions. This was qualitatively determined by plotting the historical sampled distribution of minimum aircraft miss-distances for the sector, flight-levels, and day considered. As shown by the miss-distance data in Fig. 10 there is a qualitative change in the distribution near 8NM. While the figure shows that some flights violated the minimum separation requirements of 5NM, it is assumed that errors in the miss-distances exists due to radar measurement error and interpolation error between the sampled data. Lastly, to reduce the overall complexity of the problem, only aircraft coming within 16NM of each other are considered in the conflict resolution problem.

Simulation Analysis

The simulations were performed for each of the two workload formulations, and the changes in the number of resolution commands for varying levels of the workload parameters, β and λ, were analyzed. Overall, the two different implementations return mostly similar results in regards to achieving the desired goal of limiting workload when using a semi-automated conflict resolution algorithm with a human-in-the-loop.

We first consider the results from the $CRP-\beta$ implementation. In Fig. 11, the average number of resolution commands for each aircraft are shown for various workload parameter values. It can be observed that as β is increased, the number of resolutions commands per aircraft goes up. However, while it can be concluded that limiting the number of resolutions in any 5 minute period can reduce the overall number of commands issued to an aircraft, it does not necessarily reduce the peak number of resolution commands at any time instance, as shown in Fig. 12. Therefore, the reported peak number of resolution commands at any time can remain relatively high.

As an example, for the case in which the number of resolution commands issued in a 5 minute period is limited to $\beta = 4$, it is possible that the algorithm issues all 4 commands at a single point in time. From a controllers perspective, such workload involves a stressful and difficult task. Also note that for the case $\beta = 2$, Fig. 12 indicates that at higher-traffic loads, limiting the number of resolution commands is unable to handle the traffic volume, e.g., the average peak number of commands issued in any time period is greater than $\beta = 2$. Such information can also be useful in analyzing the level of traffic that a sector can accept, given a maximum rate of issuing resolution commands based on controller limitations.

Although the results from the $CRP-\lambda$ formulation are in general similar to that of $CRP-\beta$, a smoother pattern is evident in terms of representing workload. In Fig. 13, we can observe that the number of maneuvers per aircraft increases proportionally with decreasing values of λ for each arrival rate. This proportionality appears to be mostly exponential. In addition, as shown in Fig. 14, the peak number of resolution commands per interval remains relatively low when compared with the $CRP-\beta$ formulation. Hence, the result demonstrates that by adjusting the λ parameter, not only can the average number of commands issued per aircraft decrease, but also the expected peak number of commands at any point in time. This behavior is more likely to be acceptable to a human controller.

We also compare the number of resolution com-

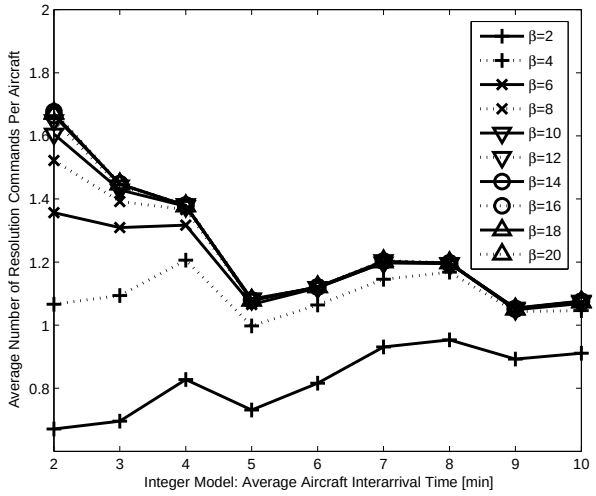

Figure 11: Workload-curves for various β according to $CRP-\beta$

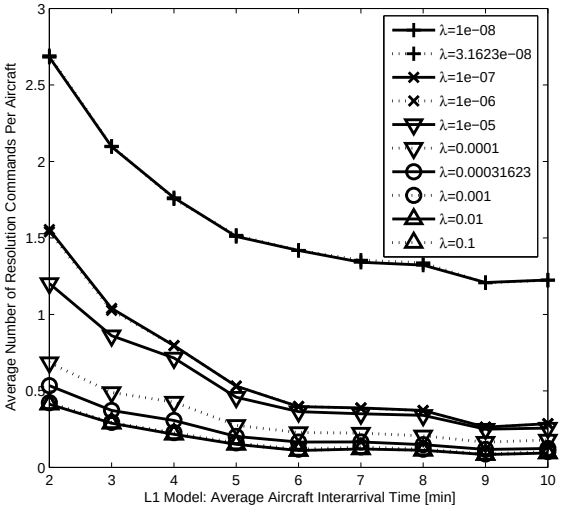

Figure 13: Workload-curves for various λ according $CRP-\lambda$

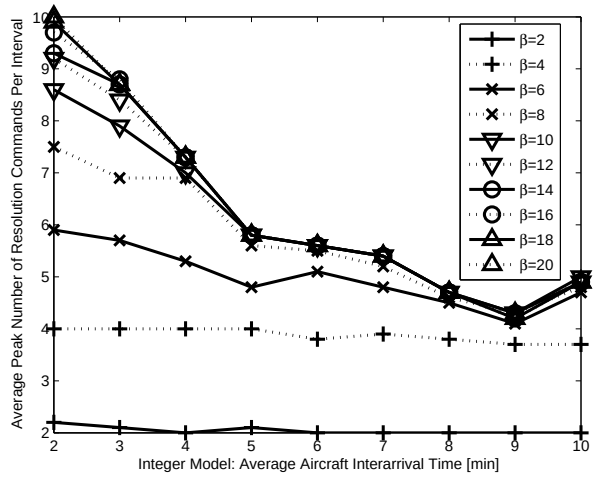

Figure 12: $CRP-\beta$: Average peak number of resolution commands required at any instance in time

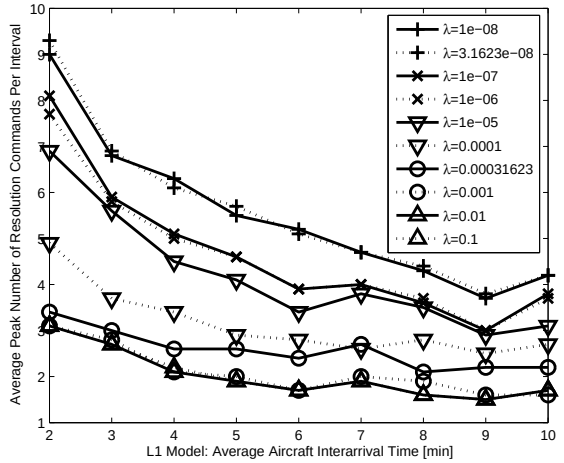

Figure 14: $CRP-\lambda$: Average peak number of resolution commands required at any instance in time

mands over any 5 minute period. Figures 15 and 16 display the corresponding curves for $CRP-\beta$ and $CRP-\lambda$, respectively. As expected, $CRP-\beta$ solutions involve lower peak number of maneuvers over a longer period of time. This is at the expense of a higher peak number of instantaneous commands issued at any resolution epoch, as discussed above. On the other hand, $CRP-\lambda$ solutions with higher λ values produce similar results, demonstrating that $CRP-\lambda$ is a more flexible formulation. While this is the case, the $CRP-\beta$ formulation provides some additional insight into the type of workload air traffic controllers should expect for a given arrival rate. It can be noted that even as the number of allowed maneuvers increases, at low traffic volumes the number of required resolutions converge. In all cases, however, as the workload parameters become more restrictive, the total number of maneuvers within a 5 minute period decreases.

Figures 17 and 18 present the average number of resolution commands issued to each aircraft for different interarrival times, as a function of the workload parameters β and λ, respectively. These plots provide

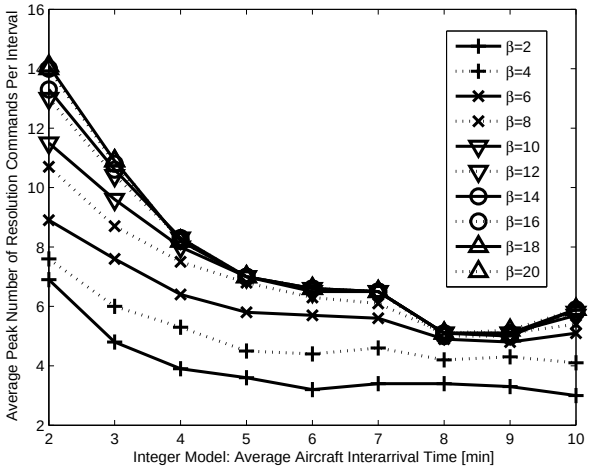

Figure 15: $CRP-\beta$**: Average peak number of resolution commands required over a 5 min period**

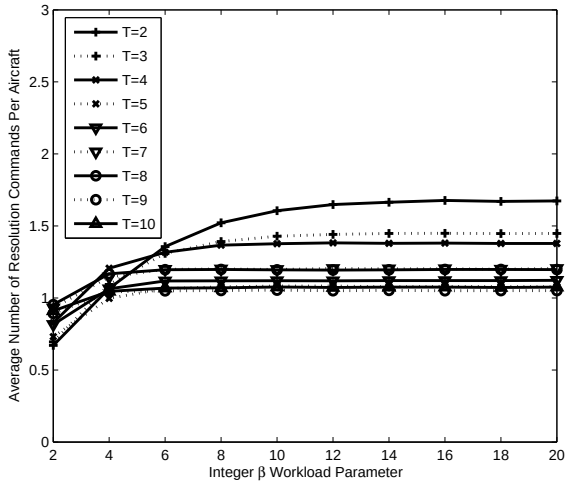

Figure 17: $CRP-\beta$**: Average number of commands per aircraft according to the workload parameter** β

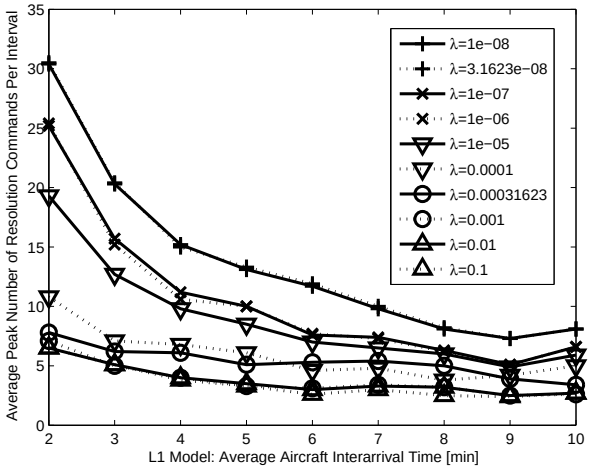

Figure 16: $CRP-\lambda$**: Average peak number of resolution commands required over a 5 min period**

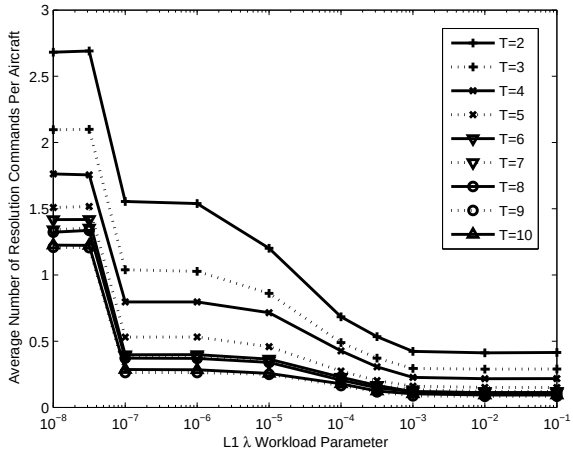

Figure 18: $CRP-\lambda$**: Average number of commands per aircraft according to the workload parameter** λ

a better representation of the sensitivity of the formulations with respect to different values of the parameters, which is likely to be significant in an empirical analysis to determine the best values of these parameters for representing controller workload. For example, in terms of the average number of maneuvers per aircraft, it can be seen that at lower values of β, the marginal effect of the parameter is similar for all arrival rates. On the other hand, similar behavior is not observed for the parameter λ, as shown in Fig. 18.

It should be noted that for all the simulations, regardless of the workload parameter, any increase in fuel burn due to conflict resolution solutions over optimal fuel-burn levels was limited to 0.5% for all traffic loads. This value is well within any uncertainty due to modeling errors in the fuel curves and wind effects. This demonstrates the value of maintaining consideration of fuel costs in conflict resolution. Furthermore, because the required minimum miss-distance is 8NM, it is actually possible to relax some of the resolution commands to achieve better fuel performance. However, this was not done in the simulations, as the objective was to represent en route traffic and controller behavior.

Conclusion and Future Work

It has been demonstrated that workload limitations can be integrated into a conflict resolution model, while still preserving fuel-cost efficiency. In fact, even as workload parameters become increasingly stringent, it is possible to maintain an acceptable trade-off with increased fuel consumption. To this end, we have presented two different parametric formulations, and performed simulations to analyze the suitability of the formulations in respecting controller workload limits. The results are promising for both formulations, and different insights can be gained from each implementation. Overall, $CRP - \lambda$ appears to be a more flexible and consistent formulation, and on average it tends to produce results that contain a higher number of total maneuvers, but lower number of simultaneous resolution commands. On the other hand, $CRP - \beta$ typically produces a less balanced set of conflict resolution maneuvers, but the resolutions typically involve a lower number of total resolution commands. Hence, given these two parametric tools, it is possible to perform an empirical analysis to identify the values of β and λ that best support the actions of a human controller.

Overall, this paper represents the first step in attempting to explicitly account for and support limitations on human decision making capabilities. This understanding will allow for the development of optimization algorithms which are better suited for implementation in decision support system.

Despite their effectiveness, the presented models involve some assumptions, and thus have some drawbacks. Because the workload and conflict resolution is only solved for instances in time, there is no concern for any conflicts and additional work that may be generated following an initial maneuver in order to return to the desired path. In fact, if exit constraints are fixed, for every initial resolution maneuver, it is expected that another maneuver will be needed. As such, there exists a probability of generating future conflicts. Also, the model does not present a method for limiting the number of commands over a given period of time, which if included could provide more flexibility in a conflict resolution formulation that considers workload constraints.

Acknowledgments

This work is funded by NASA under Grant NNX08AY52A and by the FAA under Award No.: 07-C-NE-GIT, Amendment Nos. 005, 010, and 020

References

[1] NextGen Integration and Implementation Office, "Nextgen implementation plan," tech. rep., Federal Aviation Administration, 2009.

[2] J. Villers, "En route air traffic soft management ultimate system," *ITA*, vol. 58, 2004.

[3] P. Kopardekar, J. Rhodes, A. Schwartz, S. Magyarits, and B. Willems, "Relationship of maximum manageable air traffic control complexity and sector capacity," in *26th International Congress of the Aeronautical Sciences*, 2008.

[4] E. Stein, "Air traffic controller workload: An examination of workload probe," tech. rep., Federal Aviation Administration, 1985.

[5] I. Crevits, S. Debernard, and P. Denecker, "Model building for air-traffic controllers' workload regulation," *European Journal of Operational Research*, vol. 136, no. 2, pp. 324–332, 2002.

[6] J. Kuchar and L. Yang, "A review of conflict detection and resolution modeling methods," *IEEE Transactions on Intelligent Transportation Systems*, vol. 1, pp. 179–189, Dec. 2000.

[7] L. Pallottino, E. M. Feron, and A. Bicchi, "Conflict Resolution Problems for Air Traffic Management Systems Solved With Mixed Integer Programming," *IEEE Transactions on Intelligent Transportation Systems*, vol. 3, Mar. 2002.

[8] W. Hylkema and H. Visser, "Aircraft Conflict Resolution Taking into Account Controller Workload using Mixed Integer Linear Programming," in *Proceedings of the AIAA Guidance, Navigation, and Control Conference and Exhibit*, 2003.

[9] M. Christodoulou and S. Kodaxakis, "Automatic Commercial Aircraft Collision Avoidance in Free Flight: The Three Dimensional Problem," *IEEE*

Transactions on Intelligent Transportation Systems, vol. 7, June 2006.

[10] M. Ozgur and A. Cavcar, "A knowledge-based conflict resolution tool for en-route air traffic controllers," *Aircraft Engineering and Aerospace Technology*, vol. 80, no. 6, pp. 649–656, 2008.

[11] K. Roy and C. Tomlin, "Enroute airspace control and controller workload analysis using a novel slot-based sector model," in *Proceedings of the American Control Conference*, 2006.

[12] S. Fothergill and A. Neal, "The effect of workload on conflict decision making strategies in air traffic control," *Human Factors and Ergonomics Society Annual Meeting Proceedings*, vol. 52, no. 1, pp. 39–43, 2008.

[13] A. Nuic, "Aircraft Performance Summary Tables for the Base of Aircraft Data," tech. rep., EUROCONTROL, 2004.

Email Addresses

Adan Vela: aevela@gatech.edu
Senay Solak: solak@som.umass.edu
Eric Feron: feron@gatech.edu
Karen Feigh: karen.feigh@gatech.edu
William Singhose: singhose@gatech.edu
John-Paul Clarke: johnpaul@gatech.edu

28th Digital Avionics Systems Conference
October 25-29, 2009